

# Early onset of neural synchronization in the contextual associations network

Kestutis Kveraga<sup>a,b,1</sup>, Avniel Singh Ghuman<sup>c</sup>, Karim S. Kassam<sup>d</sup>, Elissa A. Aminoff<sup>e</sup>, Matti S. Hämäläinen<sup>a,b</sup>, Maximilien Chaumon<sup>a,f</sup>, and Moshe Bar<sup>a,b,g</sup>

<sup>a</sup>Athinoula A. Martinos Center for Biomedical Imaging, Massachusetts General Hospital, Charlestown, MA 02129; <sup>b</sup>Department of Radiology, Harvard Medical School, Boston, MA 02115; <sup>c</sup>Laboratory for Brain and Cognition, National Institutes of Mental Health, Bethesda, MD 20892; <sup>d</sup>Department of Social and Decision Sciences, Carnegie Mellon University, Pittsburgh, PA 15213; <sup>e</sup>Department of Psychology, University of California, Santa Barbara, CA 93106; <sup>f</sup>Department of Psychology, Boston College, Chestnut Hill, MA 02459; and <sup>g</sup>Department of Psychiatry, Harvard Medical School, Boston, MA 02115

Edited by Robert Desimone, Massachusetts Institute of Technology, Cambridge, MA, and approved January 12, 2011 (received for review September 17, 2010)

**Objects are more easily recognized in their typical context. However, is contextual information activated early enough to facilitate the perception of individual objects, or is contextual facilitation caused by postperceptual mechanisms? To elucidate this issue, we first need to study the temporal dynamics and neural interactions associated with contextual processing. Studies have shown that the contextual network consists of the parahippocampal, retrosplenial, and medial prefrontal cortices. We used functional MRI, magnetoencephalography, and phase synchrony analyses to compare the neural response to stimuli with strong or weak contextual associations. The context network was activated in functional MRI and preferentially synchronized in magnetoencephalography (MEG) for stimuli with strong contextual associations. Phase synchrony increased early (150–250 ms) only when it involved the parahippocampal cortex, whereas retrosplenial–medial prefrontal cortices synchrony was enhanced later (300–400 ms). These results describe the neural dynamics of context processing and suggest that context is activated early during object perception.**

phase locking | oscillations | beta | visual cognition

We know from experience that specific contexts are associated with specific objects. Seeing a jumbo-sized bucket of popcorn in a movie theater would not surprise anyone familiar with American movie theaters. However, at the opera, champagne and chocolate might be the more common sight. Whether and how context can facilitate visual recognition has been the subject of much research and vigorous debate. Behavioral research studying the effects of contextual information in visual perception has shown that information about context can facilitate recognition of visual scenes and objects (1–5). However, Hollingworth and Henderson (6) have argued that at least some of this contextual facilitation is attributable to a response bias and that any contextual influence may be the result of later postidentification processes rather than early activation of contextual information during recognition (6, 7). Here, we address the central question of when in the recognition process contextual information is activated by examining the temporal dynamics of neural regions involved in processing contextual information. Furthermore, we use this information regarding the temporal dynamics of the areas involved in contextual processing to help elucidate the functions of the individual members of the context network.

In the past decade, neuroimaging studies using stimuli with strong and weak contextual associations have identified the components and basic properties of the network that mediates context-based associations; studies (8–18) have reported a core set of regions (Fig. 1A) that are activated by contextual associations: the parahippocampal cortex (PHC), the retrosplenial complex (RSC), and in some cases, the medial prefrontal cortex (MPFC). Characterizing the individual and combined roles of these regions in contextual association processing has been challenging, because the PHC, RSC, and MPFC historically have

been implicated in numerous cognitive processes. The PHC is strongly activated during scene or place recognition and spatial navigation (19), and it has been labeled the parahippocampal place area (PPA), because it is preferentially activated when one views pictures of places (20, 21). In addition, PHC has been shown to play an important role in episodic memory (22–25). These seemingly disparate roles of PHC can be reconciled if its core function is taken more globally as mediating contextual associations (8, 10, 26, 27), with spatial contextual associations processed in the PPA and nonspatial contextual associations processed in an abutting, slightly anterior region of the PHC (8, 10). In support of this view, studies have shown that the PHC response is modulated based on the degree of contextual information contained in single objects (8, 17, 27).

Similarly to the PHC, the RSC is consistently activated in tasks involving spatial navigation (28), semantic and episodic memory (29), and scene and object perception (8, 15, 30). As with the PHC, the RSC has been shown to be involved in many different cognitive processes, which makes it difficult to identify its specific function or functions (31). One possibility is that it translates allocentric representations that it receives from the hippocampus and PHC into egocentric representations (31); another possibility is that it transforms a particular instance of a context into a more generic representation of that context (8, 26, 32). The MPFC is likewise implicated in a vast number of cognitive and emotion-related functions, including semantic integration of current context, self-relevant processing, inferring mental states of others, and shifting one's perspective (17, 33–35).

Developing a better understanding of the specific roles of the PHC, RSC, and MPFC in context processing requires that we learn how these components of the context network function and interact with one another by examining the neural dynamics and communication patterns within this network and beyond. Specifically, we wanted to know when and under what conditions contextual associations (CA) modulate functional communication between the PHC, RSC, and MPFC as well as the visual cortex and possibly, other visual object processing regions, such as the fusiform and orbitofrontal cortex (36–44). Therefore, we used magnetoencephalography (MEG) to characterize the spatiotemporal dynamics and cross-cortical communication within the contextual associations network as well as with other regions involved in visual recognition. Neural oscillations play a critical role in the timing of neural events and tend to be synchronized in

Author contributions: K.S.K., E.A.A., and M.B. designed research; K.S.K. and E.A.A. performed research; K.K., A.S.G., and M.S.H. contributed new reagents/analytic tools; K.K., A.S.G., K.S.K., E.A.A., M.S.H., M.C., and M.B. analyzed data; and K.K., A.S.G., and M.B. wrote the paper.

The authors declare no conflict of interest.

This article is a PNAS Direct Submission.

<sup>1</sup>To whom correspondence should be addressed. E-mail: keastas@nmr.mgh.harvard.edu.

This article contains supporting information online at [www.pnas.org/lookup/suppl/doi:10.1073/pnas.1013760108/-DCSupplemental](http://www.pnas.org/lookup/suppl/doi:10.1073/pnas.1013760108/-DCSupplemental).

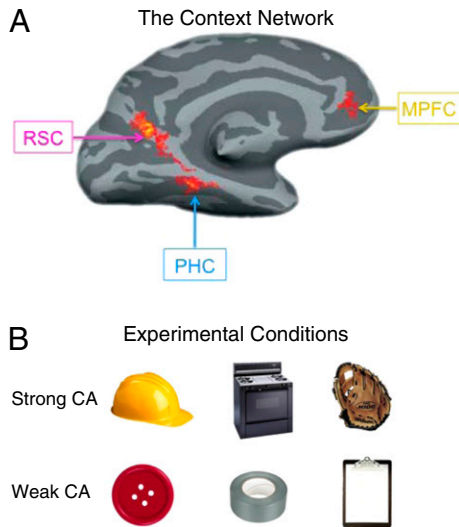


**Fig. 1.** Context network and stimuli. (A) The network of cortical regions typically activated by SCA displayed on the left hemisphere of the inflated brain surface. RSC, retrosplenial cortex; PHC, parahippocampal cortex; MPFC, medial prefrontal cortex. (B) Examples of stimuli in the SCA and WCA conditions. The SCA objects were rated as the most typical item of a particular context (e.g., construction or kitchen) by a separate survey of 35 participants. The WCA objects were rated as weakly associated with many different contexts but not strongly or consistently associated with any one context by another survey of 18 participants. The spatial frequency content of the stimuli in these two conditions did not differ (Fig. S2).

regions that exchange information (45–48). We computed phase-locking estimates to measure functional connectivity to assess whether neuronal responses in two regions have a consistently covarying phase relationship with one another (49). Unlike power estimates, which reflect the extent of synchronized neural firing, phase-locking estimates provide information about the timing of firing and interconnectivity between neural regions (50), and they are believed to be a more reliable measure of higher-level functions (51).

The behavioral paradigm that we used to investigate the dynamics of contextual association processing had been tested and used in previous functional MRI (fMRI) studies (8) in a blocked design. In the present study, we used a combination of rapid even-related design with the same stimulus set in both fMRI and MEG and used the fMRI activations to inform our region of interest (ROI) selections in MEG. We showed participants pictures of single objects with strong and weak CA (Fig. 1B) and asked them to respond through a button box when they recognized the object. The participants were not told that some objects had strong CA, whereas others had weak CA. Our hypothesis was that strong CA objects, because of their more extensive and powerful associations, should elicit increased phase locking between the core contextual and visual regions compared with weak CA objects. Finally, the timing of phase locking in the context network directly tests whether contextual information is extracted early enough to facilitate recognition, where such facilitation is useful (6).

## Results

**Behavioral Results.** The mean response time (RT) to recognize the objects in strong CA (SCA) and weak CA (WCA) conditions was very similar (SCA =  $778 \pm 504$  ms and WCA =  $773 \pm 477$  ms; paired samples  $P > 0.82$ ). Each subject's RTs were screened for outliers (2 SD above the mean) within condition. This resulted in 4.1% of trials being eliminated from the grand mean computation (3.9% for SCA and 4.3% for WCA). One subject's RT

means were a group outlier (2.47 and 2.54 SD above the group mean for SCA and WCA, respectively); however, excluding this participant's RT did not alter the relationship between SCA and WCA RT ( $623 \pm 158$  ms and  $622 \pm 205$  ms, respectively). Participants were only asked to respond when they recognized the object, and no verification or feedback as to the correctness of the response was provided; the task was not designed to test contextual facilitation. However, these results are comparable with the RTs obtained with a different cohort of subjects using a largely overlapping set of stimuli and the same task, where the SCA and WCA RTs were likewise statistically equivalent (SCA = 702 ms and WCA = 684 ms,  $P = 0.76$ ) (8). Therefore, any differences in the neural activity between SCA and WCA conditions could not be ascribed to RT and task performance differences.

**fMRI Results.** A set of ROIs (PHC, RSC, and MPFC) that we had identified a priori based on activations of contextual association processing in previous studies (8, 10, 27) showed significantly greater activation for the SCA > WCA contrast in this experiment, replicating the previous studies (Fig. S1). Given our a priori selection of the ROIs, we used the statistical threshold of  $P < 0.001$ , uncorrected, with 5-voxel extent threshold and whole-brain  $t_{1,14} = 3.79$ , which is slightly more conservative than the thresholding parameters that optimally balance Type I and Type II errors in fMRI activations ( $P < 0.005$ , uncorrected) with 10-voxel extent threshold (52). The following foci were activated above the threshold and are reported here as the group statistical peak of activation in average Montreal Neurological Institute (MNI) space coordinates: PHC ( $-30, -30, \text{and } -26$ ), RSC ( $-10, -46, \text{and } 14$ ;  $-8, -58, \text{and } 26$ ), and MPFC ( $-14, 58, \text{and } -10$ ). Other major activation clusters included the right hippocampus ( $34, -30, \text{and } -18$ ), right RSC ( $16, -56, \text{and } 18$ ), left fusiform cortex ( $-36, -42, \text{and } -14$ ), left middle occipital gyrus ( $-28, -82, \text{and } -2$ ), left ( $-40, 14, \text{and } -2$ ) and right ( $40, 20, \text{and } 2$ ) insular cortex, and left middle temporal gyrus ( $-68, -14, \text{and } 2$ ). The context network ROIs in the left hemisphere were used to anatomically guide the selection of the MEG context network ROIs used for phase-locking analysis, as described in *ROI Selection and Extraction in Methods*. The fMRI methods are described in *SI Methods*.

**MEG Phase-Locking Results.** There was stronger phase locking in the lower  $\beta$ -band for the core context regions for the SCA vs. WCA conditions (Fig. 2). Specifically, there was significantly greater phase locking in the SCA condition, occurring in the lower  $\beta$ -band between early visual regions in the occipital cortex and PHC ( $P = 0.02$ ; all MEG phase-locking  $P$  values corrected for multiple time frequency point comparisons as described in *SI Methods*). This phase locking between the occipital cortex and PHC began early, peaking between 150 and 200 ms at  $\sim 15$  Hz. Another small phase-locking cluster higher in the  $\beta$ -band ( $\sim 22$  Hz) was significant ( $P = 0.04$ ) from 200 to 220 ms. Beginning slightly later and overlapping with the occipital cortex–PHC phase locking, PHC and RSC showed significantly greater ( $P = 0.03$ ) phase locking in the SCA condition in the lower  $\beta$ -band (13–15 Hz), peaking between 170 and 240 ms. Phase locking between the occipital cortex and RSC was enhanced in the SCA condition in the later period, peaking between 310 and 360 ms ( $P = 0.03$ ) at  $\sim 15$  Hz. Phase locking of the third region in the context network, MPFC, with these regions was much weaker. PHC–MPFC did not exhibit significant phase locking ( $P = 0.62$ ), whereas RSC and MPFC showed significantly greater phase locking in the upper  $\beta$ -range only, centered at  $\sim 22$  Hz, which occurred in the later period, between 370 and 400 ms ( $P = 0.05$ ). Last, the occipital cortex and MPFC did not show significantly different phase locking ( $P = 0.27$ ). We also computed the phase angles for the significant time frequency periods in our phase-locking ROI comparisons for each subject and found that, in

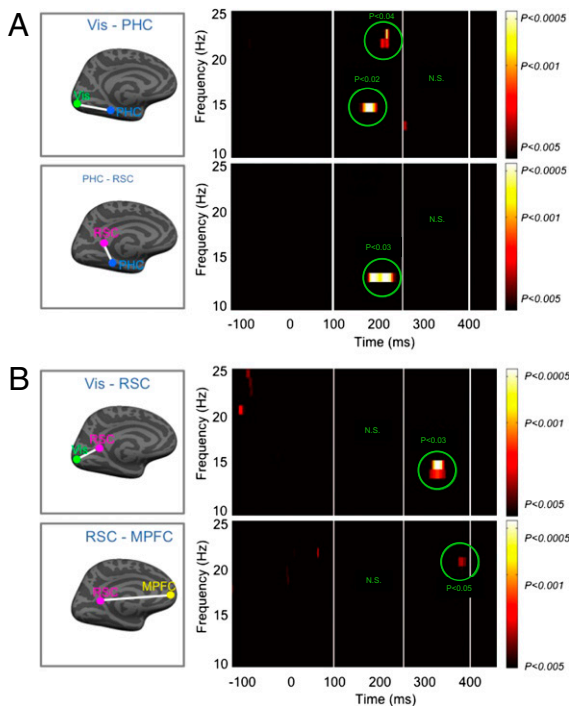


**Fig. 2.** Significant phase locking for SCA vs. WCA conditions for the core context regions and early visual cortex. *Left* is the ROI pairs showing significantly greater phase locking for SCA vs. WCA conditions. Vis, occipital cortex; PHC, parahippocampal cortex; RSC, retrosplenial complex; MPFC, medial prefrontal cortex. *Right* The color-map  $P$  values in the maps represent significance of univariate paired samples  $t$  tests between the phase-locking values for SCA and WCA conditions across subjects. The maps are not smoothed. The  $P$  values in green next to the largest clusters in each map show the statistical significance of the cluster while correcting for multiple comparisons. The correction for multiple comparisons was performed by using a nonparametric cluster permutation test (84), which is described in detail in *SI Methods*. (A) Significantly greater phase locking was seen in the early (100–250 ms) period between Vis and the PHC and between the PHC and RSC in the SCA condition relative to the WCA condition. (B) Significantly greater late (250–400 ms) phase locking was seen between the Vis and RSC and between the RSC and MPFC in the SCA condition relative to the WCA condition. *Fig. S3* also shows the reliability of MEG signal extraction from the context network regions.

virtually all cases, they were significantly different from  $0^\circ$  or  $180^\circ$ , as were the mean group phase angles. These results are reported in detail in *SI Methods*.

In contrast to the phase-locking data, local power did not differ between conditions in either the early or late time frequency bands of interest (tfBOI) in any of the context regions, as reported in detail in *SI Methods*. In addition, a trial shuffle analysis (*SI Methods*) showed that a significant residual phase locking remained after accounting for any potential coincidental phase locking to stimulus onset in the ROIs (49). Specifically, these analyses showed significant residual induced phase locking in the SCA condition between the occipital cortex and PHC from  $\sim 150$  to 200 ms ( $P = 0.014$ ) at  $\sim 15$  Hz and from  $\sim 200$  to 220 ms at  $\sim 22$  Hz ( $P = 0.046$ ), between PHC and RSC from  $\sim 170$  to 240 ms ( $P = 0.003$ ), and between the occipital cortex and RSC from  $\sim 310$  to 360 ms ( $P = 0.001$ ).

Finally, to examine whether this phase locking was specific to CA processing and the core context regions and not any object recognition-related processes and regions, we also tested phase locking between regions that we have previously observed to be activated in both fMRI and MEG during object recognition (41, 43, 44). Specifically, we additionally examined phase locking

between the fusiform and orbitofrontal cortex and between these regions and the occipital cortex, PHC, RSC, and MPFC. Critically, although these pair-wise comparisons showed increased early phase locking relative to a prestimulus baseline, this phase locking did not differ between SCA and WCA conditions. This is consistent with the more general role that the fusiform and orbitofrontal cortices play in achieving and facilitating object recognition rather than the more specialized task of activating and processing the contextual associations of visual stimuli, which is attributed to the PHC, RSC, and MPFC.

## Discussion

The primary goal of this study was to examine the temporal dynamics of the contextual association network and the communication among its components (PHC, RSC, and MPFC). We also examined the interaction of the context network regions with other regions involved in visual recognition (occipital, fusiform, and orbitofrontal cortex). We had four main findings. (i) We found significantly greater phase locking for objects with SCA than those with WCA between the PHC, RSC, and occipital cortex. (ii) This significant increase in phase locking occurred primarily in the lower  $\beta$ -band, beginning and peaking early ( $\sim 150$ – $220$  ms from stimulus onset) between the occipital cortex and PHC in the lower ( $\sim 15$  Hz) and higher ( $\sim 22$  Hz)  $\beta$ -band followed by and overlapping with PHC–RSC phase locking that occurred between 170 and 240 ms and  $\sim 13$  Hz. (iii) Greater phase locking between the occipital cortex and RSC started later, peaking between 310 and 360 ms also in the lower  $\beta$ -band ( $\sim 15$  Hz). (iv) The medial prefrontal cortex showed phase locking only with the RSC, which was weaker, relatively late ( $\sim 370$ – $400$  ms) and in the higher  $\beta$ -band ( $\sim 22$  Hz).

The pattern of phase-locking enhancement that we found for SCA stimuli compared with WCA stimuli suggests that contextual information is extracted quite early during the course of object recognition. Indeed, the timing of the interactions between the visual cortex and PHC and between the PHC and RSC (Fig. 2A) coincides with the time period when object recognition is believed to occur (43, 53–55). This early contextual activation is at odds with the proposal of a recent study that asserted that context-related activity in the PHC reflects explicit post-recognition imagining of place information (56). Instead, fMRI studies of the respective roles of the PHC and RSC suggest that the PHC is involved in extracting contextual associations from specific instances of stimuli, whereas the RSC invokes a more abstract, prototypical representation of that particular context (8, 26, 32). This period of phase locking between the PHC and RSC, thus, may reflect the translation of stimulus-specific contextual associations into a more generic context representation. Although our paradigm did not explicitly test or require contextual facilitation, the early context-based activation that we have observed is in agreement with the idea that contextual information is extracted and processed early enough for facilitating object recognition.

Later, the RSC begins phase locking with the occipital cortex at around 300 ms from stimulus onset. Generally, neural activity after about 200–300 ms has been associated predominantly with feedback processes (57, 58). Therefore, this relatively late phase locking between the RSC and occipital cortex may reflect feedback from the RSC to early visual areas. Such feedback could be seen as predictions that bias processing in the early visual regions to facilitate perception of subsequent stimuli from the same context.

The relatively late (370–400 ms) RSC–MPFC phase locking was relatively weak and therefore, should be interpreted with caution. Nevertheless, the timing (around the N400) and prefrontal involvement are consistent with reports in the event-related potential (ERP) literature ascribing such activations to integration of semantic information into the current context (59–62). In particular, the neural response 400 ms after a stimulus

steadily declines for consecutive objects or words that are contextually and semantically congruent (61). When a lexical or visual stimulus is semantically incongruent with the given context, anterior brain activity is usually more negative and posterior brain activity is more positive than for semantically congruent stimuli (60–62). Furthermore, the MPFC in particular has been implicated in the integration of semantic associations into a subjective context (17). In that study, participants were asked during a memorization task to indicate whether they remembered a given stimulus by associating it with some subjective experience (an association trial) or by noting some visual feature of the stimulus (a feature trial). They found that the MPFC (along with the PHC/hippocampus and RSC) showed greater activation for association trials than for feature trials. The stimuli encoded by forming an association were also better remembered (17). Thus, we propose that the late phase locking between the RSC and MPFC may represent the integration of the context evoked by a particular object into the current context frame.

Importantly, the timing of the phase-locking enhancement and the task in which the participants engaged (simple stimulus recognition, which did not explicitly require the activation of its context) strongly suggest that contextual associations are evoked early and automatically during object recognition rather than strictly as a postperceptual process. The timing of the significant phase locking in our study and the frequency bands in which they occurred are consistent with MEG and scalp or intracranial electroencephalography (EEG) studies investigating object recognition processes (43, 55, 63–67). Bar et al. (43) found greater phase locking between the occipital and orbitofrontal cortex and later, between the orbitofrontal and fusiform cortex when stimuli were successfully recognized rather than unrecognized. The same pattern of phase-locking enhancement was observed when the stimuli were low-pass filtered rather than high-pass filtered (magnocellular-biased low-spatial frequency stimuli have been shown to facilitate object recognition through the orbitofrontal cortex) (41, 43, 44). Similarly, Ghuman et al. (55) recently showed that facilitation of visual object recognition using repetition resulted in greater phase locking between the dorsal prefrontal and fusiform cortex, occurring between 190 and 270 ms in the low (~14 Hz)  $\beta$ -frequency band. Additionally, the earlier that this phase locking peaked, the more object recognition was facilitated. This is the same time frequency band in which SCA objects showed greater visual–PHC and PHC–RSC phase locking in the current study.

Moreover, the anatomical regions between which MEG phase locking was enhanced for the SCA vs. WCA objects are consistent with a host of fMRI studies exploring the neural substrates of contextual association processing (8, 10, 17, 27, 56). They also overlap substantially with the default mode network, as discussed in detail in Bar et al. (68). Note that no significant differences in phase locking were found between those regions and general object recognition areas (fusiform and orbitofrontal cortex), although the latter regions have exhibited significant phase-locking differences when compared under different conditions in two separate experiments (recognized vs. unrecognized and low vs. high spatial frequency objects stimuli) (43). This shows that significant phase-locking differences are task-, stimulus-, and region-specific.

What implications do these findings have for the role of context in visual object recognition? The long-running debate about the role of context in vision has split along two main types of models: (i) the so-called interactive models, which posit that context exerts influence on and can facilitate object recognition either by scene constraints on object processing (i.e., the perceptual schema models) (3, 69) or priming memory representations of context-congruent objects (i.e., priming models) (1, 4, 70), and (ii) the functional isolation model (6, 71), which maintains that object recognition and context activation are functionally separate, noninteracting processes. The conclusions that

we can draw regarding the contextual facilitation of object recognition are somewhat limited, because our paradigm was not designed to test directly whether context (e.g., supplied by a contextually congruent prime scene or word label) can facilitate recognition of a subsequently shown object. Nevertheless, the findings in this study indicate that neural communication in the context network, particularly interactions that involved PHC, differentiated between SCA and WCA objects early enough to facilitate recognition and hundreds of milliseconds before their recognition was reported through a behavioral response.

An alternative explanation for our findings could be that the SCA and WCA stimuli were somehow physically different and that these low-level differences accounted for the observed differential phase locking in the context regions. However, this is unlikely for several reasons. First, we analyzed the spatial frequency content of the stimuli in the SCA and WCA conditions and found no significant physical differences between the stimuli in these conditions (Fig. S2). Moreover, if the physical differences had accounted for the phase-locking differences between the SCA and WCA conditions, we would expect these differences to manifest themselves mostly in the low-level visual processing areas and perhaps, low- and intermediate-level object form regions in the ventral temporal lobe rather than in higher-level association regions. However, in contrast, phase synchrony differed significantly only when the relatively high-level regions specifically implicated in contextual association processing (i.e., PHC, RSC, and MPFC) were involved, and we found no significant phase-locking differences otherwise. This phase-locking sequence preferentially occurs when the stimuli with SCA bind this network together.

To conclude, the early phase-locking enhancement that we found for objects with SCA indicates that contextual information is activated early during object recognition rather than solely as a late postperceptual process. Such rapid activation of contextual associations and the ensuing facilitation of recognition make sense if one thinks of the evolutionary pressures faced by most organisms. For example, seeing a paw print or scat of a predator and rapidly activating the context associated with this image could afford the prey animal enough time for an escape, conferring it a significant evolutionary advantage over time. The brain constantly generates predictions about what it is about to perceive next (72), and activating contextual associations early during perception allows the brain to focus the gaze, attention, and action where it is most likely to yield biologically important information.

## Methods

**Participants.** Fifteen subjects participated in the fMRI study (all right-handed; eight males). Nine of fifteen subjects (five males) also participated in the MEG experiment. No participants were excluded from the study. The age range was 22–39 y, with the mean age of 25.5 y and SD of 5.5 y. All had normal or corrected to normal vision. Their informed written consent was obtained according to the procedures of the Massachusetts General Hospital Institutional Review Board and approved under Human Studies Protocols 2000P-000949 and 2002P-002035.

**Stimuli and Task.** We used color pictures of everyday objects in the two conditions of interest (SCA and WCA conditions). The object stimuli in the conditions of interest (i.e., objects with SCA and WCA) were selected on the basis of survey ratings and had been used previously (8). Briefly, the SCA and WCA items were obtained by conducting separate surveys with a separate population of subjects. All SCA objects were rated as the most typical objects of a particular context (e.g., a stove for the kitchen context) by a group of 35 subjects. Ratings from another group of 18 subjects were used to compile a list of objects that were not strongly associated with any particular context but rather, weakly associated with many different contexts (examples in Fig. 1B). Although one might wish for objects without any contextual associations as a comparison condition, in practice, real objects never appear in isolation and thus, are not devoid of any contextual associations. Therefore, the comparison in this study was between objects that should activate the context with which they are strongly associated and objects that should not

strongly activate any particular context but may weakly activate many contexts (8). In the third condition, which was included for other purposes and not analyzed in this study, abstract 2D shapes were shown. All stimuli were displayed on a gray background and spanned a maximum of  $9.2^\circ$  of visual angle. Images were displayed using the stimulus presentation package Psychtoolbox (73) running in Matlab (Mathworks) on a Macintosh Power Mac G4. The conditions comprised 53 pictures each, which were repeated three times, one in each of three sessions. Stimulus pictures appeared on the screen for 1,700 ms with a 300-ms interstimulus interval. The stimulus onsets were also randomly jittered by 0–300 ms. During MEG recording, the stimuli were projected onto a translucent screen positioned in front of the seated participant with the display resolution of  $1,024 \times 768$  pixels and a refresh rate of 75 Hz using an LP350 DLP projector (InFocus). Subjects were instructed to report when they recognized the object (in the conditions of interest) or report that the stimulus was an abstract shape. No feedback was given after the response, and subjects were unaware of the purpose of the experiment.

**MEG Methods.** The MEG was acquired with a 306-channel Neuromag Vectorview whole-head system (Elekta Neuromag Oy) comprising 204 orthogonally oriented planar gradiometers and 102 magnetometers at 102 locations. The system was housed in a three-layer magnetically shielded room (Imedco AG). To compute the head position inside the MEG dewar, four head-position indicator (HPI) electrodes were affixed to the subject's head. The positions of the HPI electrodes on the head as well as those of multiple points on the scalp were entered with a magnetic digitizer (Polhemus FastTrack 3D) in a head coordinate frame defined by anatomical landmarks, which included the nasion and the left and right auricular points. Eye blinks were monitored with four electrooculogram (EOG) sensors positioned above and beside the subjects' eyes. The MEG, EOG, and HPI sensors were sampled at 600 Hz, band pass-filtered online in the range of 0.1–200 Hz, and stored for offline analysis. Running online averages were computed to monitor and note noisy or nonfunctioning channels.

MEG data were analyzed with the MNE software package (Hämäläinen). Both the gradiometer and magnetometer data were included in the analysis. First, MEG data were screened for eye blink artifacts and low pass-filtered at 40 Hz. Trials that exceeded particular thresholds and noisy or nonfunctioning (flat) channels were eliminated from further analyses. A high-resolution structural MRI, acquired on a Siemens Allegra 3T scanner (Siemens Medical Solutions), was used to construct a forward model and visualize MEG sources. The MRI and MEG coordinates frames were coregistered using the HPI and head surface points. A single-layer boundary element model (BEM) (74) was constructed from the anatomical MRI, and it was used as a forward model to constrain MEG source location to the cortex and compute the minimum norm estimate (75) inverse solution. MEG sources were visualized on the inflated surface of the MRI (76) as dynamic statistical parametric maps (77).

**ROI Selection and Extraction.** We selected our MEG ROIs with anatomical guidance from our fMRI context network activation foci in this study, which were similar to those found in earlier fMRI studies of contextual processing (8, 27, 78). These regions included PHC, RSC, and MPFC in the left hemisphere and were verified to be reliably detectable and separable using MEG (Fig. 53). In addition, to investigate the communication between these contextual association regions and early visual regions, we also extracted raw currents from the occipital cortex site comprising ventral, medial, and polar occipital cortex. Last, two additional ROIs that had exhibited phase locking in our previous MEG experiments investigating top-down facilitation processes in object recognition (43) in fusiform and orbitofrontal cortex were included as control sites. In addition to anatomical guidance provided by the fMRI activations of the context network in this study, we also used functional

constraints, which were applied to an independent dataset as follows. We used our subjects' second run of trials to display MEG activations, which were noise-normalized dynamic statistical parametric maps (dSPMs), on each individual's inflated brain image using SCA vs. baseline comparison as our selection contrast. We drew the ROI boundaries that encompassed the peak context network activations in our fMRI experiment around MEG dSPM activations that exceeded the uncorrected dSPM threshold of  $P < 0.05$  at any time between 100 and 450 ms. We then extracted raw, minimally filtered (0.1–200 Hz) MEG currents from these ROIs in the first run of trials. Thus, the data to be used in phase-locking analysis of the contrast of interest (SCA vs. WCA objects) were (i) not functionally defined by this contrast and (ii) extracted from an independent subset of the data. Last, the interareal phase locking is, at least in principle, unrelated to the dSPM values, showing the independence of this ROI selection (79). The extracted raw currents from each ROI were submitted to phase-locking analysis as described below.

**tfBOI Selection.** Interregional communication in the upper  $\alpha$ - (10–12 Hz) and particularly, lower  $\beta$ -bands (13–25 Hz) has been found to be involved in object recognition, showing increased phase synchrony when object recognition is successful (43, 51, 55, 63–67). The  $\alpha$ -band along with the  $\theta$ -band have been thought to be involved in memory functions (50); however, the lower  $\alpha$ -band (8–9 Hz) has been found to reflect activity associated with phase-resetting, idling, or state of readiness changes, and its current role in cognitive function is unclear (80). The  $\beta$ -band, particularly the lower  $\beta$ -band, has been implicated in playing an important role in the synchronization of brain activity during object recognition (review in ref. 80). Therefore, we focused on the upper  $\alpha$ - and lower  $\beta$ -bands (10–25 Hz) in our phase-locking analyses. Because processes associated with object recognition and associative processing have been reported to occur in the poststimulus onset range of 100–450 ms (43, 55, 64, 81, 82), we constrained our statistical phase-locking analyses to the range of 100–450 ms, subdividing it into early (100–250 ms) and later (250–400 ms) periods.

**Phase-Locking Analysis.** Phase locking is a method that directly assesses the timing of oscillatory activity of the brain, irrespective of its amplitude (49, 83). The waveforms from the ROIs were filtered with a continuous Morlet wavelet transform of width 6. For the phase-locking analyses, the phase of each waveform was extracted and averaged in each trial for every frequency and time point of interest. The formula of the phase-locking value (PLV) was computed using the formula below (Eq. 1):

$$PLV(t) = \frac{1}{N} \left| \sum_{n=1}^N \exp(j(\phi_1(t, n) - \phi_2(t, n))) \right| \quad [1]$$

Here,  $t$  is the time point,  $n$  is the trial number, and  $\phi(t, n)$  is the phase of the MEG waveforms at a given time and trial in a pair of ROIs tested. The PLV measures the variability across trials of the relative phases of the two signals and can range from 0 (no phase locking) to 1 (complete phase locking). This method is functionally equivalent to the dynamic statistical parametric mapping, with the order of the wavelet filtering and the application of the inverse solution reversed relative to that method (83). We describe our statistical analyses of phase locking and power and report phase angles in *SI Methods*.

**ACKNOWLEDGMENTS.** This research was supported by National Institute of Mental Health Grant K01-MH084011 (to K.K.), National Institutes of Health Grants NS50615 and EY019477 (to M.B.), and National Science Foundation Grant 0842947 (to M.B.).

- Palmer SE (1975) The effects of contextual scenes on the identification of objects. *Mem Cognit* 3:519–526.
- Potter MC, Faulconer BA (1975) Time to understand pictures and words. *Nature* 253:437–438.
- Biederman I, Mezzanotte RJ, Rabinowitz JC (1982) Scene perception: Detecting and judging objects undergoing relational violations. *Cognit Psychol* 14:143–177.
- Bar M, Ullman S (1996) Spatial context in recognition. *Perception* 25:343–352.
- Davenport JL, Potter MC (2004) Scene consistency in object and background perception. *Psychol Sci* 15:559–564.
- Hollingworth A, Henderson JM (1998) Does consistent scene context facilitate object perception? *J Exp Psychol Gen* 127:398–415.
- Henderson JM, Hollingworth A (1999) High-level scene perception. *Annu Rev Psychol* 50:243–271.
- Bar M, Aminoff E (2003) Cortical analysis of visual context. *Neuron* 38:347–358.
- Hayes SM, Ryan L, Schnyer DM, Nadel L (2004) An fMRI study of episodic memory: Retrieval of object, spatial, and temporal information. *Behav Neurosci* 118:885–896.
- Aminoff E, Gronau N, Bar M (2007) The parahippocampal cortex mediates spatial and nonspatial associations. *Cereb Cortex* 17:1493–1503.
- Park S, Intraub H, Yi DJ, Widders D, Chun MM (2007) Beyond the edges of a view: Boundary extension in human scene-selective visual cortex. *Neuron* 54:335–342.
- Hayes SM, Nadel L, Ryan L (2007) The effect of scene context on episodic object recognition: Parahippocampal cortex mediates memory encoding and retrieval success. *Hippocampus* 17:873–889.
- Diana RA, Yonelinas AP, Ranganath C (2008) High-resolution multi-voxel pattern analysis of category selectivity in the medial temporal lobes. *Hippocampus* 18:536–541.
- Szpunar KK, Chan JC, McDermott KB (2009) Contextual processing in episodic future thought. *Cereb Cortex* 19:1539–1548.
- Aminoff E, Schacter DL, Bar M (2008) The cortical underpinnings of context-based memory distortion. *J Cogn Neurosci* 20:2226–2237.
- Gronau N, Neta M, Bar M (2008) Integrated contextual representation for objects' identities and their locations. *J Cogn Neurosci* 20:371–388.

17. Peters J, Daum I, Gizewski E, Forsting M, Suchan B (2009) Associations evoked during memory encoding recruit the context-network. *Hippocampus* 19:141–151.
18. Litman L, Awipi T, Davachi L (2009) Category-specificity in the human medial temporal lobe cortex. *Hippocampus* 19:308–319.
19. Aguirre GK, Detre JA, Alspop DC, D'Esposito M (1996) The parahippocampus subserves topographical learning in man. *Cereb Cortex* 6:823–829.
20. Epstein R, Kanwisher N (1998) A cortical representation of the local visual environment. *Nature* 392:598–601.
21. Epstein R, Harris A, Stanley D, Kanwisher N (1999) The parahippocampal place area: Recognition, navigation, or encoding? *Neuron* 23:115–125.
22. Gabrieli JDE, Keane MM, Zarella MM, Poldrack RA (1997) Preservation of implicit memory for new associations in global amnesia. *Psychol Sci* 8:326–329.
23. Wagner AD, et al. (1998) Building memories: Remembering and forgetting of verbal experiences as predicted by brain activity. *Science* 281:1188–1191.
24. Ranganath C, et al. (2004) Dissociable correlates of recollection and familiarity within the medial temporal lobes. *Neuropsychologia* 42:2–13.
25. Daselaar SM, Fleck MS, Cabeza R (2006) Triple dissociation in the medial temporal lobes: Recollection, familiarity, and novelty. *J Neurophysiol* 96:1902–1911.
26. Bar M (2004) Visual objects in context. *Nat Rev Neurosci* 5:617–629.
27. Bar M, Aminoff E, Schacter DL (2008) Scenes unseen: The parahippocampal cortex intrinsically subserves contextual associations, not scenes or places per se. *J Neurosci* 28:8539–8544.
28. Maguire EA (2001) The retrosplenial contribution to human navigation: A review of lesion and neuroimaging findings. *Scand J Psychol* 42:225–238.
29. Svoboda E, McKinnon MC, Levine B (2006) The functional neuroanatomy of autobiographical memory: A meta-analysis. *Neuropsychologia* 44:2189–2208.
30. Henderson JM, Larson CL, Zhu DC (2008) Full scenes produce more activation than close-up scenes and scene-diagnostic objects in parahippocampal and retrosplenial cortex: An fMRI study. *Brain Cogn* 66:40–49.
31. Vann SD, Aggleton JP, Maguire EA (2009) What does the retrosplenial cortex do? *Nat Rev Neurosci* 10:792–802.
32. Park S, Chun MM (2009) Different roles of the parahippocampal place area (PPA) and retrosplenial cortex (RSC) in panoramic scene perception. *Neuroimage* 47:1747–1756.
33. Raichle ME, et al. (2001) A default mode of brain function. *Proc Natl Acad Sci USA* 98:676–682.
34. Buckner RL, Carroll DC (2007) Self-projection and the brain. *Trends Cogn Sci* 11:49–57.
35. Mason MF, et al. (2007) Wandering minds: The default network and stimulus-independent thought. *Science* 315:393–395.
36. Thorpe SJ, Rolls ET, Maddison S (1983) The orbitofrontal cortex: Neuronal activity in the behaving monkey. *Exp Brain Res* 49:93–115.
37. Tanaka K (1996) Inferotemporal cortex and object vision. *Annu Rev Neurosci* 19:109–139.
38. Logothetis NK, Sheinberg DL (1996) Visual object recognition. *Annu Rev Neurosci* 19:577–621.
39. Rolls ET (2000) Functions of the primate temporal lobe cortical visual areas in invariant visual object and face recognition. *Neuron* 27:205–218.
40. Haxby JV, et al. (2001) Distributed and overlapping representations of faces and objects in ventral temporal cortex. *Science* 293:2425–2430.
41. Bar M, et al. (2001) Cortical mechanisms specific to explicit visual object recognition. *Neuron* 29:529–535.
42. Rolls ET (2004) The functions of the orbitofrontal cortex. *Brain Cogn* 55:11–29.
43. Bar M, et al. (2006) Top-down facilitation of visual recognition. *Proc Natl Acad Sci USA* 103:449–454.
44. Kveraga K, Boshyan J, Bar M (2007) Magnocellular projections as the trigger of top-down facilitation in recognition. *J Neurosci* 27:13232–13240.
45. Singer W (1999) Neuronal synchrony: A versatile code for the definition of relations? *Neuron* 24:49–65.
46. Varela F, Lachaux JP, Rodriguez E, Martinerie J (2001) The brainweb: Phase synchronization and large-scale integration. *Nat Rev Neurosci* 2:229–239.
47. Buzsáki G, Draguhn A (2004) Neuronal oscillations in cortical networks. *Science* 304:1926–1929.
48. Fries P (2005) A mechanism for cognitive dynamics: Neuronal communication through neuronal coherence. *Trends Cogn Sci* 9:474–480.
49. Lachaux JP, Rodriguez E, Martinerie J, Varela FJ (1999) Measuring phase synchrony in brain signals. *Hum Brain Mapp* 8:194–208.
50. Klimesch W, Freunberger R, Sauseng P, Gruber W (2008) A short review of slow phase synchronization and memory: Evidence for control processes in different memory systems? *Brain Res* 1235:31–44.
51. Düzel E, Neufang M, Heinze HJ (2005) The oscillatory dynamics of recognition memory and its relationship to event-related responses. *Cereb Cortex* 15:1992–2002.
52. Lieberman MD, Cunningham WA (2009) Type I and Type II error concerns in fMRI research: Re-balancing the scale. *Soc Cogn Affect Neurosci* 4:423–428.
53. VanRullen R, Thorpe SJ (2001) The time course of visual processing: From early perception to decision-making. *J Cogn Neurosci* 13:454–461.
54. Rousselet GA, Macé MJ, Thorpe SJ, Fabre-Thorpe M (2007) Limits of event-related potential differences in tracking object processing speed. *J Cogn Neurosci* 19:1241–1258.
55. Ghuman AS, Bar M, Dobbins IG, Schnyer DM (2008) The effects of priming on frontal-temporal communication. *Proc Natl Acad Sci USA* 105:8405–8409.
56. Epstein RA, Ward EJ (2010) How reliable are visual context effects in the parahippocampal place area? *Cereb Cortex* 20:294–303.
57. Tomita H, Ohbayashi M, Nakahara K, Hasegawa I, Miyashita Y (1999) Top-down signal from prefrontal cortex in executive control of memory retrieval. *Nature* 401:699–703.
58. Garrido MI, Kilner JM, Kiebel SJ, Friston KJ (2007) Evoked brain responses are generated by feedback loops. *Proc Natl Acad Sci USA* 104:20961–20966.
59. Düzel E, et al. (1999) Task-related and item-related processes in episodic and semantic retrieval: A combined PET and ERP study. *Proc Natl Acad Sci USA* 96:1794–1799.
60. Ganis G, Kutas M (2003) An electrophysiological study of scene effects on object identification. *Brain Res Cogn Brain Res* 16:123–144.
61. Hagoort P (2008) The fractionation of spoken language understanding by measuring electrical and magnetic brain signals. *Philos Trans R Soc Lond B Biol Sci* 363:1055–1069.
62. Sitnikova T, Holcomb PJ, Kiyonaga KA, Kuperberg GR (2008) Two neurocognitive mechanisms of semantic integration during the comprehension of visual real-world events. *J Cogn Neurosci* 20:2037–2057.
63. Tarkoh L (2009) EEG oscillations induced by contour closure in a noisy visual field. *Behav Brain Res* 196:55–62.
64. Sehatpour P, et al. (2008) A human intracranial study of long-range oscillatory coherence across a frontal-occipital-hippocampal brain network during visual object processing. *Proc Natl Acad Sci USA* 105:4399–4404.
65. Okazaki M, Kaneko Y, Yumoto M, Arima K (2008) Perceptual change in response to a bistable picture increases neuromagnetic beta-band activities. *Neurosci Res* 61:319–328.
66. Supp GG, et al. (2005) Semantic memory retrieval: Cortical couplings in object recognition in the N400 window. *Eur J Neurosci* 21:1139–1143.
67. von Stein A, Rappelsberger P, Sarnthein J, Petsche H (1999) Synchronization between temporal and parietal cortex during multimodal object processing in man. *Cereb Cortex* 9:137–150.
68. Bar M, Aminoff E, Mason M, Fenske M (2007) The units of thought. *Hippocampus* 17:420–428.
69. Boyce SJ, Pollatsek A (1992) Identification of objects in scenes: The role of scene background in object naming. *J Exp Psychol Learn Mem Cogn* 18:531–543.
70. Ullman S (1996) *High-Level Vision: Object Recognition and Visual Cognition* (MIT Press, Cambridge, MA).
71. Hollingworth A, Henderson JM (1999) Object identification is isolated from scene semantic constraint: Evidence from object type and token discrimination. *Acta Psychol (Amst)* 102:319–343.
72. Bar M (2007) The proactive brain: Using analogies and associations to generate predictions. *Trends Cogn Sci* 11:280–289.
73. Pelli DG (1997) The VideoToolbox software for visual psychophysics: Transforming numbers into movies. *Spat Vis* 10:437–442.
74. Hämäläinen MS, Sarvas J (1989) Realistic conductivity geometry model of the human head for interpretation of neuromagnetic data. *IEEE Trans Biomed Eng* 36:165–171.
75. Hämäläinen MS, Hari R (2002) Magnetoencephalographic characterization of dynamic brain activation: Basic principles and methods of data collection and source analysis. *Brain Mapping: The Methods*, eds Toga AW, Mazziotta JC (Academic, San Diego), 2nd Ed, pp 227–254.
76. Fischl B, Sereno MI, Dale AM (1999) Cortical surface-based analysis. II: Inflation, flattening, and a surface-based coordinate system. *Neuroimage* 9:195–207.
77. Dale AM, et al. (2000) Dynamic statistical parametric mapping: Combining fMRI and MEG for high-resolution imaging of cortical activity. *Neuron* 26:55–67.
78. Bar M, Aminoff E, Ishai A (2008) Famous faces activate contextual associations in the parahippocampal cortex. *Cereb Cortex* 18:1233–1238.
79. Kriegerkorte N, Simmons WK, Bellgowan PS, Baker CI (2009) Circular analysis in systems neuroscience: The dangers of double dipping. *Nat Neurosci* 12:535–540.
80. Uhlhaas PJ, Haenschel C, Nikolić D, Singer W (2008) The role of oscillations and synchrony in cortical networks and their putative relevance for the pathophysiology of schizophrenia. *Schizophr Bull* 34:927–943.
81. Vanni S, Revonsuo A, Saarinen J, Hari R (1996) Visual awareness of objects correlates with activity of right occipital cortex. *Neuroreport* 8:183–186.
82. Tallon-Baudry C, Bertrand O (1999) Oscillatory gamma activity in humans and its role in object representation. *Trends Cogn Sci* 3:151–162.
83. Lin FH, et al. (2004) Spectral spatiotemporal imaging of cortical oscillations and interactions in the human brain. *Neuroimage* 23:582–595.
84. Maris E, Oostenveld R (2007) Nonparametric statistical testing of EEG- and MEG-data. *J Neurosci Methods* 164:177–190.